Finite Element Modeling of PVDF Matrix Carbon Fiber Composites

MICHAEL A. GREMINGER and GHAZALEH HAGHIASHTIANI

ABSTRACT

Self-sensing carbon fiber reinforced composites have the potential to enable structural health monitoring that is inherent to the composite material rather than requiring external or embedded sensors. It has been demonstrated that a self-sensing carbon fiber reinforced polymer composite can be created by using the piezoelectric polymer polyvinylidene difluoride (PVDF) as the matrix material and using a Kevlar layer to separate two carbon fiber layers. In this configuration, the electrically conductive carbon fiber layers act as electrodes and the Kevlar layer acts as a dielectric to prevent the electrical shorting of the carbon fiber layers. This composite material has been characterized experimentally for its effective d_{33} and d_{31} piezoelectric coefficients. However, for design purposes, it is desirable to obtain a predictive model of the effective piezoelectric coefficients for the final smart composite material. Also, the inverse problem can be solved to determine the degree of polarization obtained in the PVDF material during polarization by comparing the effective d_{33} and d_{31} values obtained in experiment to those predicted by the finite element model. In this study, a coupled piezoelectric-mechanical finite element modeling approach is used to predict the mechanical and piezoelectric performance of a plain weave carbon fiber reinforced PVDF composite.

SMART COMPOSITE MATERIAL PROPERTIES AND EXPERIMENTAL CHARACTERIZATION

In this section, the methods used for fabrication and polarization of the composite material are briefly explained. In addition, results from experimental characterization of mechanical and piezoelectric properties of the material are presented. More details on fabrication, polarization, and experimental

Michael A. Greminger, Dept. of Mechanical and Industrial Engineering, University of Minnesota Duluth, 1305 Ordean CT, Duluth, MN 55812, U.S.A.
Ghazaleh Haghiashtiani, Dept. of Mechanical Engineering, University of Minnesota, 111 Church ST SE, Minneapolis, MN 55455, U.S.A.

characterization of the proposed composite structure can be found in an earlier work published by the authors [1].

Fabrication and Polarization Procedure

The reinforcement materials used for fabricating the proposed composite structure were two layers of carbon fiber and one layer of Kevlar fabric between them. Due to the electrical conductivity of carbon fiber material, these layers also acted as the electrodes for polarization and sensing purposes, which were separated from each other by the Kevlar dielectric layer. As shown in Figure 1(a), two layers of PVDF film between each of the reinforcement layers and on the top and bottom formed the matrix of the composite structure. Since the characterization of the proposed smart composite involved tensile tests, extra layers of Kevlar and PVDF were added to the main structure of the composite to prevent the potential pressure introduced to the samples by the grips of the tensile test equipment (see Figure 1(a)). The final samples (see Figure 1(b)) were made by melt curing the stack of materials at 200 ºC for 4 hours under a pressure of 7 kpa.
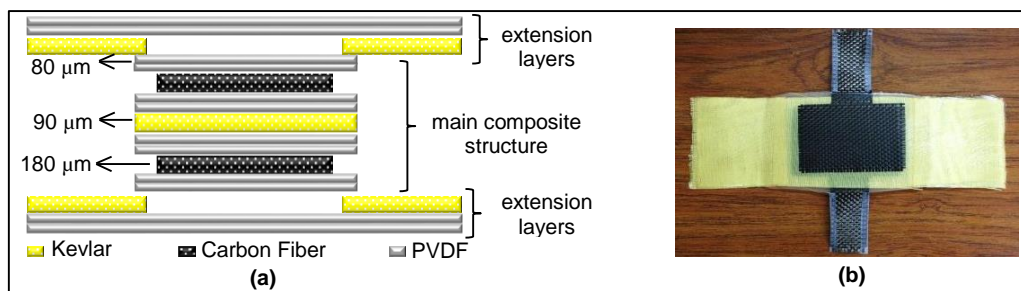

Figure 1. Structure of the proposed composite material. Cross sectional view of materials' stack-up and thicknesses before melt curing (a) and top view of final samples after melt curing (b).

The next step in preparing the smart composite structure was polarization to ensure the alignment of dipoles in PVDF matrix. Due to the structure of the proposed composite, the common methods used for polarization of PVDF material were not feasible and special considerations were required. For instance, applying high electric fields would result in dielectric break down and stretching the composite was impractical due to the high stiffness of carbon fiber and Kevlar layers. To overcome these limitations, a 2^3 full factorial design of experiment (DOE) was implemented to find the optimal condition of three factors (temperature, voltage, and duration of polarization) used in the polarization process. The experiments were performed at two levels of each of the factors. For each experiment, the effectiveness of polarization condition was evaluated in tensile tests as the ratio of the charge developed in the composite structure to the force applied to it. The analysis of the results showed that for the tested conditions, polarizing the samples by applying 2000 V at 75 ºC for duration of 20 minutes would yield the highest degree of polarization and sample response.

Mechanical Characterization

For the purpose of mechanical characterization, the Young's modulus of the composite structure was evaluated. Tensile load was applied to the composite material using MTS equipment and the resulting strain was recorded with an extensometer, which was attached to the samples. This test was replicated for different samples and with extensometer attached at opposing sides to ensure that samples were not bending. Analyzing the obtained stress-strain plots yielded an average Young's modulus of 21.9 Gpa for the proposed composite structure. It should be noted that the experimental elastic modulus given here differs from the value previously published [1] due to a change in the width dimension used in calculating the average stress. The width of the carbon fiber layers is used here rather than the entire width since the carbon fiber layers dominate the stiffness of the structure.

Piezoelectric Characterization

The effective piezoelectric coefficients d_{31} and d_{33} were experimentally determined in tensile and compression tests, respectively. In each case, a cyclic load was applied to the samples and the charge developed in the smart composite material due to the applied load was extracted. The effective piezoelectric coefficient could then be calculated as:

$$(d_{3i})_{eff} = \frac{Q/A_{CF,electrode}}{\sigma_{Average_i}} \quad \textit{(for i=1 or 3)} \tag{1}$$

where Q represents the charge developed in the composite structure due to the applied load, $A_{CF, electrode}$ is the area of carbon fiber electrode layer, and $\sigma_{Average}$ is the average stress over the structure in either the 1 direction for d_{31} or in the 3 direction for d_{33} where the 3 direction is the thickness direction of the composite structure. The results obtained from piezoelectric characterization of the proposed composite material are summarized in Table I. As it can be seen, the experimental characterization yielded the effective d_{31} and d_{33} coefficients of $4.36\,\mathrm{e}^{-4}\,\frac{pC/m^2}{N/m^2}$ and $1.95\,\frac{pC/m^2}{N/m^2}$, respectively. These values differ from those previously published [1] since the average stress over the entire structure is used here, where in the previous results only the stress in the layer between the carbon fiber layers was used. This change was made to match the computation of the effective piezoelectric coefficients obtained from the finite element analysis discussed below.

TABLE I. SUMMARY OF THE RESULTS OBTAINED FROM EXPERIMENTAL
PIEZOELECTRIC CHARACTERIZATION OF COMPOSITE STRUCTURE

	Experimental d_{31}	Experimental d_{33}
Total force	15.90 N	176 N
Charge developed in the composite	0.480 pC	0.235 nC
Effective piezoelectric coefficient	$4.36\,\mathrm{e}^{-4}\,\frac{pC}{N}$	$1.95\,\frac{pC}{N}$

SOLID MODEL AND FINITE ELEMENT MESH REPRESENTATION OF COMPOSITE STRUCTURE

Optical cross section images of the actual smart composite structures were used determine the dimensions of the carbon fiber and Kevlar tows. These dimensions, along with a cross section image of the actual composite, are shown in Figure 2. Using these dimensions, a solid model was constructed of the composite. In order to use the fewest elements in the finite element mesh, the smallest repeating pattern in the carbon fiber weave was used to size the solid model. This resulted in a solid model with a length and width of 4.2 mm and a height of 1.08 mm. The carbon fiber and Kevlar components of the solid model are shown in Figure 3. Figure 4 shows the finite element mesh generated from this solid model. A tetrahedral mesh with mid-side nodes was used.
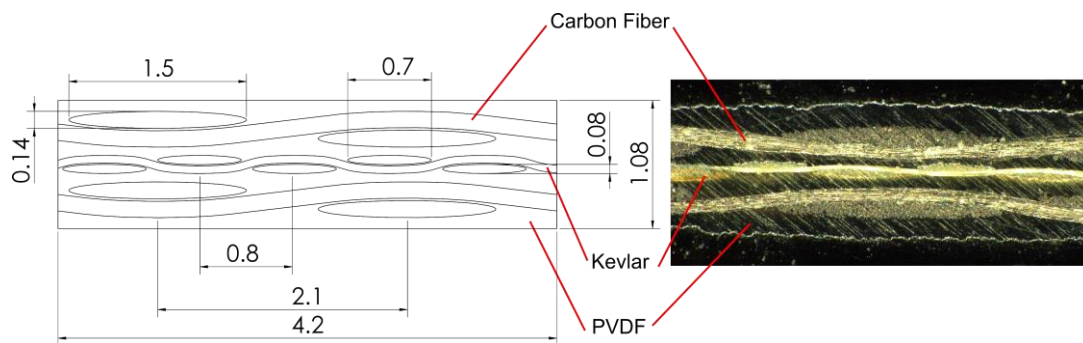

Figure 2. Dimensions in mm used for solid model on left and cross section of actual composite on right.
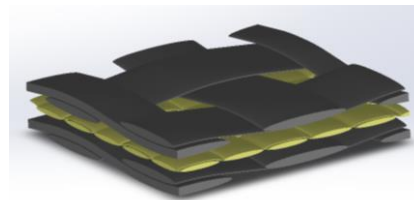

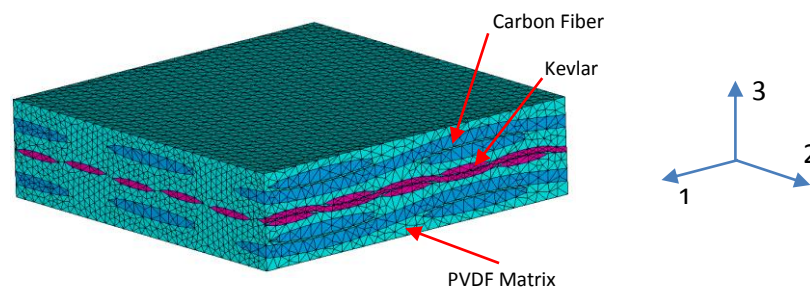Figure 3. Solid model of carbon fiber and Kevlar weaves (PVDF matrix not shown).

Figure 4. Finite element mesh of composite structure. The three direction is the direction of poling.

MICROMECHANICS FOR THE ELECTROMECHANICAL PROPERTIES OF THE CARBON FIBER AND KEVLAR TOWS

The smart composite structure is a multi-scale composite. The carbon fiber and Kevlar weaves, as shown in the previous section, are at the millimeter scale. However, the carbon fiber and Kevlar tows are composed of numerous micron scale fibers. Figure 5 shows a scanning electron microscope (SEM) image of a portion of one of the carbon fiber tows showing the numerous fibers surrounded by PVDF matrix that make up each of the tows.

One approach to model the properties for each of the tows would be to include the geometry of the carbon and Kevlar fibers in the finite element model. However, this would result in a finite element mesh with more elements then could solved in a reasonable amount of time since the Kevlar fibers are 15 µm in diameter and the carbon fibers are 6 µm in diameter, both of which are three orders of magnitude smaller than the carbon fiber weave. Fortunately, for a continuous matrix composite, the electrical, mechanical, and piezoelectric properties can be computed numerically based on the elecromechanical properties of the constituent materials [2].

The coupled piezoelectric and mechanical equations can be expressed as [3]:

$$\begin{bmatrix} \sigma_{11} \\ \sigma_{22} \\ \sigma_{33} \\ \sigma_{23} \\ \sigma_{13} \\ \sigma_{12} \\ D_1 \\ D_2 \\ D_3 \end{bmatrix} = \begin{bmatrix} C_{11} & C_{12} & C_{12} & 0 & 0 & 0 & 0 & 0 & e_{31} \\ C_{12} & C_{22} & C_{23} & 0 & 0 & 0 & 0 & 0 & e_{32} \\ C_{13} & C_{23} & C_{33} & 0 & 0 & 0 & 0 & 0 & e_{33} \\ 0 & 0 & 0 & C_{44} & 0 & 0 & 0 & e_{24} & 0 \\ 0 & 0 & 0 & 0 & C_{55} & 0 & e_{15} & 0 & 0 \\ 0 & 0 & 0 & 0 & 0 & C_{66} & 0 & 0 & 0 \\ 0 & 0 & 0 & 0 & e_{15} & 0 & \kappa_1 & 0 & 0 \\ 0 & 0 & 0 & e_{24} & 0 & 0 & 0 & \kappa_2 & 0 \\ e_{31} & e_{32} & e_{33} & 0 & 0 & 0 & 0 & 0 & \kappa_3 \end{bmatrix} \begin{bmatrix} \epsilon_{11} \\ \epsilon_{22} \\ \epsilon_{33} \\ 2\epsilon_{23} \\ 2\epsilon_{13} \\ 2\epsilon_{12} \\ E_1 \\ E_2 \\ E_3 \end{bmatrix} \qquad (2)$$

where C are the components of the elastic stiffness matrix, e are the piezoelectric coefficients in stress form, κ are the orthotropic dielectric permittivity constants, σ respresents the stress components, D are the components of electric displacement, ϵ are the components of strain, and E are the electric field components. The matrix in (2) is the electromechanical material matrix for the material. Each constituent material in the continuous fiber composite will have its own matrix. The combined electromechanical material matrix for the composite is obtained by combining the material matrices of the constituent materials in a weighted fashion. Dunn and Taya [2], [4] provide a theoretical means to combine these material matrices where the relative weighting is provided by integral equations that are numerically integrated. The Dunn and Taya method was implemented as part of this work in order to compute the electromechanical material matrices for the carbon fiber and Kevlar tows that form the smart composite structure.

The weighting of the electromechanical material matrices depends on the volume fraction of fibers in the composite. The volume fraction for both the carbon fiber and Kevlar tows were computed from SEM images. Figure 5 shows one image that was used to compute the volume fraction of carbon fibers. Several SEM images were used in computing the carbon fiber and Kevlar volume fractions yielding an

average carbon fiber volume fraction of 55% and an average Kevlar volume fraction of 61%.
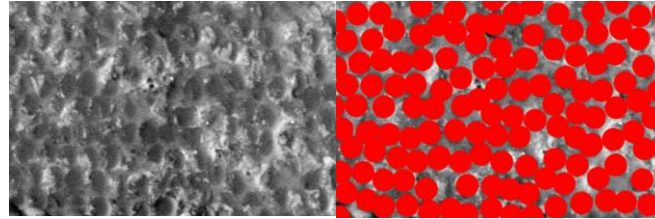

Figure 5: SEM image of carbon fiber tow cross section on left and manually placed dots representing fiber locations on right.

With the volume fractions computed, the composite electromechanical material matrix can be computed for the carbon fiber and Kevlar tows. The constituent materials properties used in computing the tow properties are summarized in Table II. Since the goal of this study is to determine the degree of poling achieved in the PVDF component of the composite, multiple values for the PVDF piezoelectric coefficients were modeled, as will be discussed in the following section.

TABLE II. MATERIAL PROPERTIES USED FOR CONSTITUENT MATERIALS

Material	Elastic Modulus (GPa)	Poisson's Ratio	Relative Permittivity
PVDF	1.72 [5]	0.34 [6]	9.3 [5]
Kevlar	83 [7]	0.44 [7]	3.7 [8]
Carbon Fiber	228 [7]	0.25 [7]	-

The results of applying the Dunn and Taya method to the Kevlar tows are shown in Figures 6 and 7. For the tows, the 1 direction is aligned with the fibers and the poling direction is the 3 direction. The Dunn and Taya elastic moduli were compared to the elastic moduli obtained using the modified rule of mixtures [7]. The E_{11} direction elastic modulus values are indistinguishable between the two methods and the two methods are very close for the E_{33} direction elastic modulus.
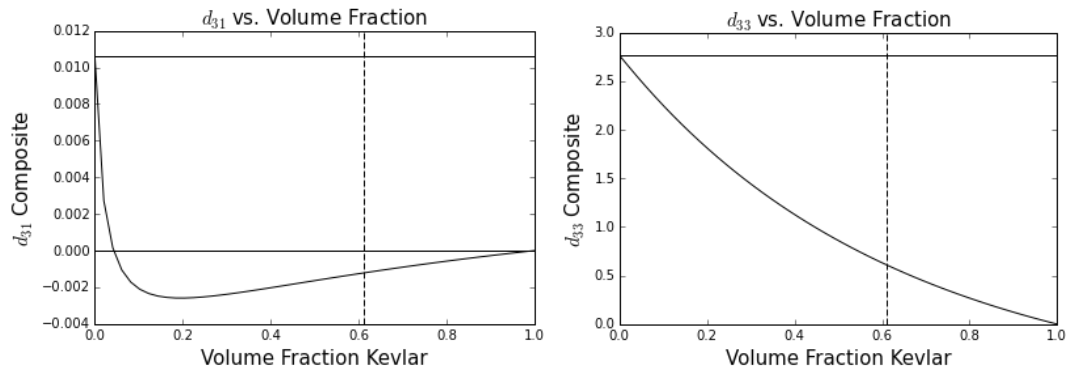

Figure 6: Piezoelectric coefficients versus Kevlar volume fraction for Kevlar tows.
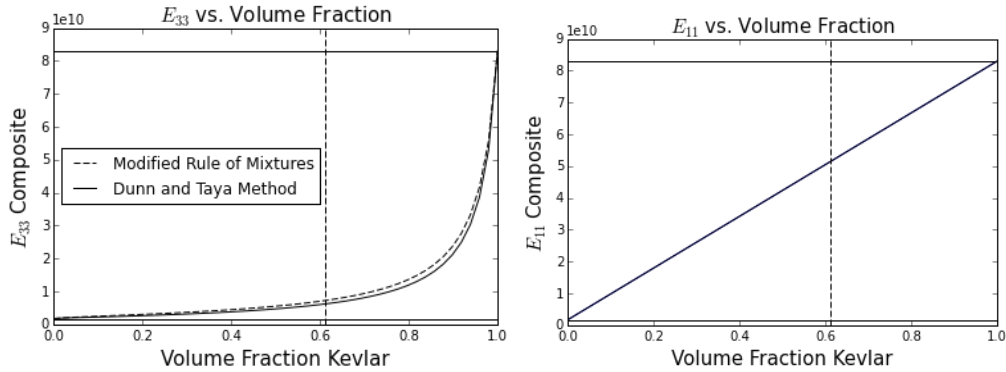
Figure 7: Elastic modulus components versus Kevlar volume fraction for Kevlar tows.

FINITE ELEMENT ANALYSIS

Using the eletromechanical material matrices for the carbon fiber and Kevlar tows obtained using the Dunn and Taya method, the smart composite material was modeled using the finite element mesh from Figure 4. ANSYS was used to perform the modeling using the SOLID227 electrical-mechanical coupled field element type. The elastic moduli and piezoelectric coefficients were obtained using boundary conditions that mimic those used in the experiments discussed above. In addition, the capacitance of the composite structure was modeled. The coordinate system is shown in Figure 4 where the 3 direction is the poling direction of the composite structures.

Since the main aim of the finite element modeling was to determine the degree of polarization obtained in the PVDF component of the composite, a 2^2 factorial modeling DOE was performed where all possible combinations of two levels of PVDF d_{31} and d_{33} were modeled. A quadratic response surface was fit to the DOE results and the values of the PVDF piezoelectric coefficients required to obtain the effective piezoelectric coefficients obtained from experiment were determine. Using this technique, it was determined that a PVDF d_{31} of 0.01 pC/N and a PVDF d_{33} of 2.7 pC/V were required to obtained the experimental effective piezoelectric coefficients of the smart composite structure. Using these PVDF piezoelectric coefficients, Table III summarizes the finite element modeling results and compares those results to the experimental measurements of the composite structure.

TABLE III. COMPARISON OF FINITE ELEMENT AND EXPERIMENTAL SMART COMPOSITE PROPERTIES

Source	d_{31} (pC/N)	d_{33} (pC/N)	E_{11} (GPa)	Capacitance (pF)
Experiment	.00044	1.95	21.9	585
Finite Element Model	.00031	1.97	20.9	489

CONCLUSIONS

Table III summarizes the results of the finite element modeling of the smart composite structure. As would be expected, there is good agreement between the modeled and experimental piezoelectric values since the PVDF piezoelectric coefficients in the model were chosen to match the experimental values. There is also fairly good agreement with the elastic modulus and capacitance values.

Through finite element modeling of the smart composite structure, it was found that the polarization process obtains a PVDF component d_{31} value of 0.01 pC/N and a d_{33} value of 2.7 pC/N. The d_{31} value obtained is about three orders of magnitude smaller than would be expected for a fully polarized PVDF material [9] and the d_{33} value is about one order of magnitude smaller than would be expected for a fully polarized PVDF material [9]. This indicates that there is opportunity increase the sensitivity of the proposed smart composite structure by at least an order of magnitude by improving the polarization process. Also, the disproportionally low d_{31} value indicates that the crystal structure of the PVDF phase may not match the crystal structure normally obtained in polarized PVDF structures. An investigation of the crystalline structure may be pursued in future work to characterize the polarization of the PVDF in a similar fashion to what has been done in other studies [10].

References

1. G. Haghiashtiani and M. A. Greminger. 2015. "Fabrication, polarization, and characterization of PVDF matrix composites for integrated structural load sensing," *Smart Mater. Struct.*, 24(4):045038.
2. M. L. Dunn and M. Taya. 1993. "An Analysis of Piezoelectric Composite Materials Containing Ellipsoidal Inhomogeneities," *Proc. Math. Phys. Sci.*, 443(1918):265–287.
3. G. M. Odegard. 2004. "Constitutive modeling of piezoelectric polymer composites," *Acta Mater.,* 52(18): 5315–5330.
4. M. L. Dunn and M. Taya. 1993. "Micromechanics predictions of the effective electroelastic moduli of piezoelectric composites," *Int. J. Solids Struct.*, 30(2):161–175.
5. "Professional Plastics, PVDF Film - Material Data Sheet." [Online]. Available: http://www.professionalplastics.com/professionalplastics/content/PVDFFilmDataSheet.doc.
6. T. Furukawa, J. X. Wen, K. Suzuki, Y. Takashina, and M. Date. 1984. "Piezoelectricity and pyroelectricity in vinylidene fluoride/trifluoroethylene copolymers," *J. Appl. Phys.*, 56(3):829–834.
7. L. P. Kollár and G. S. Springer. 2003. *Mechanics of composite structures*. Cambridge University Press.
8. M. L. Minges. 1989. *Electronic materials handbook: packaging*, vol. 1. ASM International.
9. T. R. Dargaville, M. C. Celina, J. M. Elliott, P. M. Chaplya, G. D. Jones, D. M. Mowery, R. A. Assink, R. L. Clough, and J. W. Martin. 2005. "Characterization, performance and optimization of PVDF as a piezoelectric film for advanced space mirror concepts," Sandia National Laboratories.
10. M. T. Riosbaas, K. J. Loh, G. O'Bryan, and B. R. Loyola. 2014 "In situ phase change characterization of PVDF thin films using raman spectroscopy," *Proc. of SPIE Vol. 9061*.